Title:

Phytochemical Analysis, and Antioxidant and Hepatoprotective Activities of *Chamaerops humilis* L. Leaves; A Focus on Xanthine Oxidase

Authors and affiliations:

Shimaa A. Ahmed[a], Emadeldin M. Kamel[a*], Ayman M. Mahmoud[b], Hamdi M. D. Nasr[c], Hossam M. Hassan[d], Mohammed M. Alanazi[e], Mostafa E. Rateb[d], Walaa G. Hozayen[f], Sayed A. Ahmed[a]

[a]Department of Chemistry, Faculty of Science, Beni-Suef University, Beni-Seuf, 62514, Egypt.

[b]Department of Life Sciences, Faculty of Science and Engineering, Manchester Metropolitan University, Manchester M1 5GD, UK.

[c]Department of Chemistry, Faculty of Science, Al-Azhar University (Assiut), Assiut, 71524, Egypt.

[d]Department of Pharmacognosy, Faculty of Pharmacy, Beni-Suef University, Beni-Suef, 62514, Egypt.

[e]Department of Pharmaceutical Chemistry, College of Pharmacy, King Saud University, Riyadh 11451, Saudi Arabia

[f]Department of Biochemistry, Faculty of Science, Beni-Suef University, Beni- Seuf, 62514, Egypt.

Corresponding author:
Emadeldin M. Kamel
Department of Chemistry, Faculty of Science, Beni-Suef University, Beni-Seuf, 62514, Egypt.
emad.abdelhameed@science.bsu.edu.eg

Abstract

Chamaerops humilis L. is clumping palm of the family *Arecaceae* with promising health-promoting effects. Parts of this species are utilized as food and employed in folk medicine to treat several disorders. This study investigated the phytochemical constituents of *C. humilis* leaves and their antioxidant and xanthine oxidase (XO) inhibitory activities *in vitro* and *in vivo* in acetaminophen (APAP)-induced hepatotoxicity in rats. The chemical structure of the isolated phytochemicals was determined using data obtained from UV, MS, IR, and ^{1}H-, ^{13}C-NMR spectroscopic tools as well as comparison with authentic markers. Eleven compounds, including tricin 7-O-β-rutinoside, vicenin, tricin, astragalin, borassoside D, pregnane-3,5,6,16-tetrol, oleanolic acid, β-sitosterol and campesterol were isolated from *C. humilis* ethanolic extract (CHEE). CHEE and the butanol, n-hexane, and dichloromethane fractions exhibited *in vitro* radical scavenging and XO inhibitory efficacies. The computational findings revealed the tendency of the isolated compounds towards the active site of XO. *In vivo*, CHEE ameliorated liver function markers and prevented tissue injury induced by APAP in rats. CHEE suppressed hepatic XO, decreased serum uric acid and liver malondialdehyde (MDA), and enhanced reduced glutathione (GSH), superoxide dismutase (SOD), and catalase in APAP-treated rats. CHEE ameliorated serum tumor necrosis factor alpha (TNF-α) and interleukin (IL)-1β in APAP-treated rats. Thus, *C. humilis* is rich in beneficial phytochemicals that possess binding affinity towards XO. *C. humilis* exhibited potent *in vitro* antioxidant and XO inhibitory activities, and prevented APAP hepatotoxicity by attenuating tissue injury, oxidative stress and inflammation.

Keywords: Palm; Oxidative stress; Hepatotoxicity; Xanthine oxidase.

1. Introduction

Palms have yielded bioactive secondary metabolites, substantiating their efficacy in traditional therapeutic practices. Many palm species have been recently shown to contain substantial levels of phytoconstituents with beneficial biological and health-promoting effects [1]. Antioxidant properties, enzyme inhibition activities, and hepatoprotective, anti-inflammatory, and spermatogenesis-enhancing effects are among the reported efficacies of different palm species [1-2]. *Chamaerops humilis* L. (*C. humilis*) is a shrub-like clumping palm of the family *Arecaceae*, with multiple stems emerging from a common base [3]. It is a dwarf shrub commonly growing in north Africa and south Europe where it is mostly cultivated as an ornamental because of its decorative characteristics [4]. Traditionally, many parts of the plant are used in folk medicine and some parts are consumed as food. The leaves are used for the treatment of diabetes in both Algeria and Morocco and the husk, fruits, and young suckers are consumed as food in the south of Spain, Morocco, and Italy, respectively. The fruits have a bitter taste and are therefore used as an astringent and the palm heart is utilized traditionally for the therapeutic use against digestive disorders [1c, 5]. Therefore, *C. humilis* is valuable as a food source and for the treatment of many disorders.

Previously reported phytochemical investigations on *C. humilis* revealed the isolation of phenolic acids, flavonoids, spirostanyl glycoside, saponins, terpenes, alkaloids, and volatile compounds [6]. The extract of *C. humilis* leaves exhibited radical-scavenging activity (RSA) and inhibited lipoxygenases (LOXs) [7]. These activities show that *C. humilis* could be beneficial against oxidative stress (OS)-related disorders. Elevated concentrations of reactive oxygen species (ROS) result in OS, contributing to the damage of cellular lipids, proteins, and DNA. ROS can provoke an inflammatory response by activating nuclear factor-kappaB (NF-κB), leading to the release of different inflammatory mediators and cytokines which work in coordination with ROS to elicit cell death in different organs, such as the liver and kidney [8]. For instance, OS is centrally implicated in liver injury induced by the analgesic acetaminophen

(APAP) [9]. The sources of ROS in APAP toxicity include the mitochondria, cytochrome P450, and immune cells [9]. In addition, there is a recent interest in the role of xanthine oxidase (XO) in APAP-induced liver damage [9]. XO catalyzes the generation of uric acid by oxidation of hypoxanthine and xanthine, but its activity is associated with the production of ROS (Battelli et al. 2016). The involvement of XO-mediated ROS in drug hepatotoxicity has been acknowledged [9-10], and the preventive influence of the XO inhibitor allopurinol against APAP-induced OS in the liver of mice has been reported by Jaeschke et al [10].

Despite the demonstrated beneficial effects of *C. humilis*, nothing has yet been reported on its inhibitory efficacy on XO and its potential protective role against APAP-induced liver injury. Accordingly, this study investigated the phytoconstituents of *C. humilis* and its antioxidant and XO inhibitory activities *in vitro* as well as in a rodent model of APAP hepatotoxicity *in vivo*. Moreover, the binding affinity of *C. humilis* phytoconstituents towards XO was studied by molecular docking.

2. Material and methods

2.1. Phytochemical investigation

2.1.1. General

Silica gel 60 GF_{254} plates from E. Merck were employed for thin-layer chromatography (TLC) analysis. Vacuum liquid chromatography (VLC) was conducted using E. Merck's silica gel 60 with a mesh size of 0.04-0.063 mm. Column chromatographic analysis involved the use of Silica gel 60, Sephadex LH20, and polyamide 6S from E. Merck. ,^{1}H and ^{13}C-NMR spectral data were measured in a JEOL-JNM-EX-400 spectrometer. EI-MS data were recorded with a JEOL JMS-700T mass spectrometer. HR-MS data were and estimated using a Thermo Instruments MS system (LTQ XL/LTQ Orbitrap Discovery) coupled to a Thermo Instruments

HPLC system (Accela PDA detector, Accela PDA autosampler, and Accela pump). HPLC separations were carried out using a Phenomenex C18 column (5 µm, 100 Å, 10 × 250 mm), connected to an Agilent 1200 series binary pump, and monitored by means of Agilent photodiode array detector.

2.1.2. Plant material

The Leaves of *C. humilis* (*Arecaceae*) used in this study were collected during the period from March 2011 to February 2013 from a mature tree growing in Orman botanical Garden (latitude - longitude: 30.02904 - 31.21263, Cairo, Egypt). After the validation of the species' authenticity by botanists from the Botany Department at Beni-Suef University, Egypt, a voucher specimen (No.: BSU-CH2012-327) was meticulously archived in the Herbarium of the Faculty of Science (Registration code: BSU- HERB412564).

2.1.3. Extraction and isolation

The dried grounded leaves of *C. humilis* (2 Kg) were exhaustively extracted by cold maceration using 70% ethanol (EtOH; 3×4 L) at room temperature. The solvent was then removed under reduced pressure to produce a dark brown sticky mass of the crude extract (300 g). This extract was then dissolved in 500 mL water and successively partitioned with n-hexane, followed by dichloromethane (DCM) and *n*-butanol to afford three main fractions weighing 13, 5.7, and 50 g, respectively. A polyamide column chromatography was employed to chromatograph the *n*-butanol fraction (30g) which was eluted with water-methanol (H_2O-MeOH) gradient to yield 8 subfractions (B1-B8). Subfraction B1 (7.5 g) was further chromatographed over the C18 column eluted with H_2O-MeOH gradient to afford compound **1** (170 mg). Subfraction B2 (190 mg) was further purified using Sephadex LH-20 eluted with 20% MeOH to give nine subfraction (B2.1-B2.9). subfractions B2.1-B2.3 were collected and combined depending on their TLC profile, then the combined fractions were additionally purified over Sephadex-LH20

column using 20% EtOH as an eluent to produce the purified compounds **2** (18 mg) and **3** (5mg). Subfractions B2.4-B2.9 were combined and subjected to fractionation over Sephadex LH-20 column and subjected to LC/HRSEI-MS analysis to afford compounds **4-7.** the combined subfractions were repeatedly chromatographed over Sephadex LH-20 using methanol as an eluent to afford compounds **4** (15 mg), **5** (17 mg), **6** (11 mg) and **7** (8 mg).

The DCM fraction underwent Vacuum Liquid Chromatography (VLC) on a silica gel column, employing a DCM-MeOH gradient elution, resulting in the production of four subfractions (D1-D4). The constituents of subfractions D1 and D2 were identified by LC/HRSEI-MS analysis to confirm the existence of compounds **8** and **9**. These compounds were isolated from repeatedly chromatographing subfractions D1 and D2 over silica gel column using the system DCM-MeOH of increasing polarity as an eluent to afford 16 subfractions (S1-S16). Subfractions S4-S11 were combined according to similar TLC R_f values and spot color and subjected to purification over a silica gel column using the same eluent of decreasing polarity to finally afford the purified compounds **8** (14 mg) and **9** (16 mg).

The *n*-hexane fraction (6g) was subjected to a saponification process to isolate saponifiable (0.3g) and unsaponifiable (3g) fractions, then the unsaponifiable fraction was subjected to VLC on silica gel 60 column chromatography eluted with *n*-hexane/EtOAc of gradient elution to yield two subfractions (H1-H2) weighing 40 and 20 mg, respectively. Each subfraction was repeatedly chromatographed over Sephadex LH-20 column using *n*-hexane-DCM (1:1) as an eluent to afford the purified compounds **10** (10 mg) and **11** (17 mg), respectively.

2.2. *In silico* molecular docking analysis

Density Functional Theory (DFT) calculations employed in this investigation were executed by means of Gaussian 09 software package [11]. The geometrical structures of *C. humilis* isolated phytochemicals were fully optimized at the B3LYP level of theory without constrains

[12] employing the 6-311G (d, p) basis set [13]. The original 3D pdb X-ray crystal structure of XO was downloaded from the protein data bank (PDB ID: 3NVY). The original pdb structures of various drugs were generated using UCSF Chimera software [14]. The molecular docking analysis was conducted using Autodock Tools (ADT) version 1.5.6 and the AutoDock Vina software packages [15]. ADT software was used to optimize the pdb structures of different ligands for the docking run. The PyMOL v2.3.2 software was utilized for the evaluation of molecular recognition, screening of binding modes, and the assessment of ligand-enzyme interactions. The 3D crystal structure of XO underwent preparation for the docking run through ADT software. This optimization process encompassed the removal of water and nonstandard amino acid residues, the addition of polar hydrogens, and configuring the grid box to align with the active site amino acid residues [16].

2.3. *In vitro* radical scavenging activity (RSA) and XO-inhibitory activity of *C. humilis*

2.3.1. DPPH RSA activity

The RSA properties of *C. humilis* extract and butanol, DCM, and *n*-hexane fractions were assayed according to Cheel et al [17]. Briefly, different concentrations of the samples were incubated with 0.1 mM solution of DPPH in methanol for 30 min and the absorbance was measured at 517 nm. Ascorbic acid was employed as a positive control.

2.3.2. XO inhibitory activity

The XO inhibitory activity of *C. humilis* extract and its fractions was assayed by mixing different concentrations with xanthine (0.05 mM), sodium phosphate buffer (50 mM), and XO followed by incubation for 0.5 hour at 37°C. 3.2% perchloric acid was added to cease the reaction and equivalent volumes of the mixture and copper (II) chloride (10 mM) and neocuproine (7.5 mM) and double volume of ammonium acetate (1 M). The mixture was then stored for 30 min and absorbance was recorded at 450 nm [18].

2.4. *In vivo* hepatoprotective, antioxidant, and anti-inflammatory activities of *C. humilis*

2.4.1. Experimental animals and treatments

Adult male Wistar rats (160-180 g), sourced from the National Research Centre's animal facility in Giza, Egypt, were kept in standard conditions (temperature 23±1°C and humidity 50-60%). These rats were provided with unrestricted access to food and water. Following a one-week acclimatization period, the rats were divided into three groups (n = 6) as outlined below:

Group I (Control): received the vehicle.

Group II (APAP): received 2000 mg/kg APAP.

Group III (APAP + CHEE): received 2000 mg/kg APAP and 200 mg/kg CHEE.

APAP and CHEE were dissolved in 0.5% CMC and administered via oral gavage. CHEE was administered for 7 days and APAP on day 7. The dose of APAP was selected based on the study of Chellappan et al [19]. The leaves extract of palm showed beneficial effects in diabetic rats at doses of 200 and 400 mg/kg [20] and therefore the 200 mg/kg was selected in this study. 48 h after APAP, blood was collected via cardiac puncture under ketamine anesthesia and the animals were immediately dissected. Liver samples were homogenized (10% w/v) in Tris-HCl buffer (pH 7.4) and the homogenate was centrifuged, and the clear supernatant was kept at -80°C. Other samples were collected on 10% neutral-buffered formalin (NBF) for histopathology. The experiment was approved by the Animal Care and Use Committee of Beni-Suef University (200312).

2.4.2. Biochemical assays

Alanine transaminase (ALT), alkaline phosphatase (ALP), and aspartate aminotransferase (AST) activities, and albumin levels were determined in serum using kits obtained from Bio-Diagnostic (Egypt). Malondialdehyde (MDA) and reduced glutathione (GSH) levels, and

superoxide dismutase (SOD) and catalase activities were assayed in the liver of rats using kits supplied by Bio-Diagnostic (Egypt). XO activity was determined in serum and liver using a reagent kit supplied by Solarbio (China). Serum tumor necrosis factor (TNF)-α and interleukin (IL)-1β were assayed using ELISA kits (Cusabio, China).

2.4.3. Histopathology

Liver samples were fixed in 10% NBF for 24 h, dehydrated, cleared, and then embedded in paraffin. Five µm sections were cut using a microtome and then stained hematoxylin and eosin (H&E) [21].

2.4.5. Statistical analysis

The data were analyzed using the one-way ANOVA followed by Tukey's test on GraphPad 8. A P value <0.05 was considered significant and the data are represented as mean ± SEM.

3.1. Results

3.1. Phytochemical study

The phytochemical investigation of various fractions of *C. humilis* revealed the isolation of 11 known compounds (Fig. 1). The identification of the structures of isolated phytochemicals relied on data obtained from UV, MS, IR, and ^{1}H-, ^{13}C-NMR spectroscopic tools as well as comparison with authentic markers. The isolated compounds were elucidated as tricin 7-*O*-*β*-rutinoside (**1**) [6c], vicenin (**2**) [22], tricin (**3**) [23], astragalin (**4**) [24], borassoside D (**5**) [25], pregnane-3,5,6,16-tetrol (**6**) [26], 3'-Hydroxy-4'-O-methyldaidzein- 7-O-[2E-butenoyl-(→6)-*β*-D-glucopyranoside] (**7**), 9,14- Dihydroxy octadecanoic acid methyl ester (**8**) [27], oleanolic acid (**9**) [28], β-sitosterol (**10**) [29] and campesterol (**11**) [30].

3.2. *In vitro* radical scavenging and XO inhibitory activities of *C. humilis*

The RSA activity of *C. humilis* and its fractions was evaluated using the DPPH test. The crude extract showed the most potent DPPH RSA with IC_{50} of 45.90 µg/ml followed by the DCM fraction (IC_{50} = 62.93 µg/ml), butanol (IC_{50} = 80.39 µg/ml) and n-hexane (IC_{50} = 138.77 µg/ml) fractions as represented in Fig. 2A-D. Ascorbic acid showed a concentration-dependent RSA with IC_{50} of 28.92 µg/ml (Fig. 2E). Likewise, XO inhibitory activity of the crude extract and fractions was investigated *in vitro*. The crude extract showed the highest inhibitory activity (IC_{50} = 44.99 µg/ml), followed by butanol (IC_{50} = 54.70 µg/ml), DCM (IC_{50} = 56.51 µg/ml), and *n*-hexane fractions (IC_{50} = 79.39 µg/ml) (Fig. 3A-D). Allopurinol exhibited an IC_{50} value of 1.99 µg/ml (Fig. 3E).

3.3. *In silico* molecular docking analysis

Herein, we reported the binding modes of *C. humilis* isolated compounds with XO through molecular docking analysis. Table 1 displays the binding affinities, potential polar bonding, and hydrophobic interactions between the target enzyme and the isolated phytochemicals as determined by AutoDock Vina. Figures 4 and 5 represent the binding interactions of most potent phytochemicals isolated from *C. humilis* with XO. Compound **1** exhibited the lowest binding affinity (-9.7 kcal/mol) followed by compound **7** (-8.7 kcal/mol) and compound **3** (-8.4 kcal/mol) (Fig. 4A). The interactions of compounds **1**, **7**, and **3** are shown in Fig. 4B, 5A, and 5B, respectively.

3.4. *In vivo* hepatoprotective, antioxidant, and anti-inflammatory activities of *C. humilis*

Given that the crude extract (CHEE) exhibited the most potent RSA and XO inhibitory activity, we evaluated its antioxidant and anti-inflammatory efficacies in a rat model of APAP hepatotoxicity. Microscopic examination (Fig. 6A) of the control rats revealed normal structure of the liver tissue whereas APAP caused tissue injury manifested by vacuolations, inflammatory cell injury, and hemorrhage. Rats that received CHEE showed nearly normal

tissue architecture with normal hepatocytes, central vein, and sinusoids (Fig. 6A). The hepatotoxic effect of APAP and the beneficial role of CHEE were supported by the biochemical findings (Fig. 6B-E). APAP-treated animals showed a significant increase in serum ALT (Fig. 6B), AST (Fig. 6C), and ALP (Fig. 6D) activities ($P<0.001$) and decreased albumin (Fig. 6E; $P<0.001$). These effects were reversed in CHEE-treated rats ($P<0.001$). APAP significantly increased liver MDA (Fig. 7A) whereas GSH (Fig. 7B), SOD (Fig. 7C), and catalase (Fig. 7D) were declined ($P<0.001$). Hepatic XO activity (Fig. 8A) and serum uric acid (Fig. 8B) were elevated in APAP-administered rats ($P<0.001$). CHEE effectively decreased MDA, XO, and uric acid and enhanced GSH, SOD, and catalase. In addition, CHEE decreased serum levels of TNF-α and IL-1β in APAP-treated rats ($P<0.001$; Fig. 8C-D).

4. Discussion

This study investigated the phytochemical constituents, RSA, XO inhibitory efficacy, and hepatoprotective effect of *C. humilis*. Eleven phytoconstituents were isolated from the plant extract which with its fractions showed *in vitro* free radical and XO inhibition. *In silico* findings revealed the binding affinities of the phytoconstituents against XO and *in vivo* studies showed the antioxidant, anti-inflammatory and hepatoprotective efficacies of CHEE.

The leading cause of liver failure in many nations is attributed to the hepatotoxic effects of APAP [31]. OS is an imbalance between ROS production and the ability of the antioxidant defenses to neutralize them [32]. It is implicated in different metabolic disorders and drug-induced hepatotoxicity [32]. Therefore, agents with radical scavenging properties can mitigate ROS generation and prevent the negative impact of OS on cellular macromolecules [32]. In this study, *C. humilis* extract and its fractions exhibited potent RSA revealed by the results of the DPPH test. In addition, CHEE and the fractions exhibited inhibitory activity against XO, a molybdenum-containing enzyme that produces ROS and its high activity is associated with OS

in several disorders, including APAP hepatotoxicity [9-10, 33]. These findings indicated the antioxidant properties of *C. humilis* with the highest activity shown by the crude extract (CHEE), an effect that is attributed to the presence of more phytoconstituents than in the fractions. Accordingly, the antioxidant properties of various parts of *C. humilis* have been demonstrated by Gonçalves et al [1c] using DPPH and other assays. The results of Gonçalves et al [1c] indicated the rich flavonoid content of the leaves. Flavonoids have a strong ability to combat free radicals mainly by scavenging free radicals [34]. Here, 11 compounds were isolated from the leaves of *C. humilis*, demonstrating its rich content of flavonoids and sterols.

XO inhibitory activities of *C. humilis* isolated phytochemicals (**1**-**11**) were studied by molecular docking assessments. The stabilities of the formed drug-enzyme complexes are mainly dependent on the number of formed polar bonds, hydrophobic interactions and drug-enzyme binding energies [35]. Particularly, polar bonding is a driving factor responsible for the binding of drugs into the main binding cavity of the enzymes [36]. These polar interactions play a significant role in molecular characterization, drug affinities, and drug-enzyme configuration [16]. Another major factor that contributes significantly to the binding of a drug to the enzyme's active site is the hydrophobic binding interaction, the ligand's lipophilic surface and the protein binding pocket hydrophobic amino acid residues [24a, 36b]. Thus, for a stable drug-enzyme interaction, a proper geometrical alignment between the ligand and the binding cavity of the enzyme is crucial [37]. The low binding affinity values of the tested compounds suggest a strong binding potential of these compounds to XO active site. The binding interaction of compound **1** indicated robust polar bonding and hydrophobic interactions within the active site of XO. Similarly, the docking poses of compounds **7** and **3** revealed extensive interactions that likely contribute to their inhibitory effects. Notably, compounds **1**, **4**, and **7** displayed the highest extent of polar bonding among the tested compounds. These interactions are crucial as they often enhance binding affinity and specificity by facilitating stronger and more stable enzyme-

inhibitor complexes [36a]. The docking analysis also uncovered a dense network of hydrophobic interactions within the XO binding site for all tested phytochemicals. This network is essential for the stabilization of the enzyme-inhibitor complex. Additionally, a high extent of phenylalanine residues was detected in the binding mechanism of the inhibitors. These residues are capable of forming thermodynamically favorable π-π interactions, further stabilizing the binding of the inhibitors to the enzyme. The molecular docking results showed that the tested inhibitors predominantly occupied the main binding site of XO. This observation is significant as it indicates that these phytochemicals may effectively compete with the natural substrates of XO, thereby inhibiting its activity. The compatibility of these compounds to the XO active site is estimated from the existence of these key residues in the main active site of the complex formed. Hence, the molecular docking analysis of phytochemicals isolated from *C. humilis* with XO revealed that several compounds, particularly compounds **1**, **7**, and **3**, exhibit strong binding affinities and significant interactions within the enzyme's active site. The presence of polar and hydrophobic interactions, along with π-π interactions involving phenylalanine residues, suggests that these compounds could serve as potent inhibitors of XO. Further experimental validation is required to confirm these computational findings and to explore their potential therapeutic applications.

Subsequently, we assessed the antioxidant and hepatoprotective capabilities of CHEE in a rat model subjected to APAP-induced hepatotoxicity, emphasizing the involvement of XO. The induction of liver injury by APAP is widely acknowledged as a prominent and extensively investigated model for evaluating plant-based therapeutics and other interventions targeting liver protection.[9]. Here, APAP-treated rats exhibited liver injury manifested by the histopathological alterations, including hydropic degeneration in the hepatocytes, hemorrhage, inflammatory cell infiltration and congestion. Additionally, circulating aminotransferases were increased and albumin was decreased, denoting hepatocyte injury. ALT, AST, and ALP are

enzymes found within hepatocytes and the increase in their activities in the blood is a marker of hepatocyte damage. Albumin is a protein synthesized by the liver and its low blood levels indicate hepatocyte dysfunction and/or damage. Accordingly, investigators have demonstrated increased serum aminotransferases and decreased albumin along with histopathological alterations in the liver of rodents following APAP administration [38]. CHEE prevented liver injury and ameliorated serum aminotransferases and albumin in APAP-administered rats. Given the implication of OS in the hepatotoxic mechanism of APAP [9], The hepatoprotective effectiveness of CHEE can be directly ascribed to its antioxidative characteristics.

Excessive ROS and OS play an essential role in hepatocyte injury caused by APAP [9]. Here, APAP resulted in an elevation of MDA levels and a reduction in GSH as well as antioxidant enzyme activities, indicating the occurrence of OS. One important factor contributing to the toxicity is the process of metabolic activation of APAP, catalyzed by cytochrome P450. This process produces NAPQI, which is a reactive metabolite responsible for initiating toxicity [39]. Overdosing on APAP leads to the excessive production of NAPQI, which results in GSH depletion. This causes the creation of adducts on proteins, including those found in mitochondria. Additionally, it triggers OS, mitochondrial dysfunction, breakage of nuclear DNA, and the death of cells by necrosis, followed by an inflammatory reaction. This response involves the production of pro-inflammatory cytokines and the activation of immune cells [39]. Accordingly, the levels of TNF-α and IL-1β were markedly elevated in the liver of APAP-treated rats in this study. Lipid peroxidation (LPO) is a process induced by ROS and has been implicated in liver injury under OS conditions [8a, 8d, 24a, 40]. MDA is a marker of LPO and its increase in the injured tissue indicates LPO. Wendel et al [41] have pinpointed the involvement of LPO in the mechanism underlying APAP hepatotoxicity for the first time. P450-mediated metabolism releases ROS which initiates LPO and the use of P450 inhibitors suppressed APAP-induced hepatic LPO and liver injury in mice [42]. CHEE demonstrated significant *in*

vivo antioxidant activity by effectively inhibiting LPO and enhancing GSH levels along with antioxidant enzyme activities. The antioxidant efficacy of CHEE aligns with the *in vitro* findings and could be directly connected to its rich content of antioxidant phytoconstituents. Plants rich in polyphenols, particularly flavonoids, have shown potent antioxidant and hepatoprotective activities [8a, 24a, 36a, 43]. Despite a wealth of data indicating the presence of generalized OS during APAP-induced hepatotoxicity, there is ongoing controversy regarding the specific cellular or intracellular sources and the nature of ROS in this context.[9]. The role of cytochrome P450, mitochondria, and immune cells as sources of ROS in APAP hepatotoxicity has been extensively described. Moreover, the role of XO as a potential source of ROS in drug hepatotoxicity has been acknowledged [9-10]. In this context, inhibitors of XO can represent a valuable source for the prevention and/or attenuation of APAP-induced OS and liver injury. Accordingly, Jaeschke et al [10] have reported the protective effect of the XO inhibitor allopurinol against OS induced by APAP in the liver of mice. In the current study, CHEE decreased liver XO activity along with serum uric acid levels. The XO inhibitory activity of CHEE contributed, at least in part, to its antioxidant and hepatoprotective efficacies. The results of this investigation revealed the potent radical-scavenging, XO inhibitory, antioxidant, anti-inflammatory, and hepatoprotective effects of *C. humilis*. The use of a single dose of CHEE and the lack of a group treated with a standard drug could be considered as limitations. However, this study represents a step in delineating the hepatoprotective role of *C. humilis*.

5. Conclusion

C. humilis is a valuable source of phytochemicals with radical-scavenging, XO inhibitory, and hepatoprotective activities. *C. humilis* extract and its fractions showed RSA and inhibited XO activity *in vitro*. The *in silico* results showed the binding affinity of *C. humilis* phytoconstituents towards XO. *C. humilis* extract conferred protection against APAP

hepatotoxicity by preventing tissue injury, OS, and inflammatory response, and boosting antioxidants in the liver of rats. Besides the *in vitro* studies, *C. humilis* extract attenuated XO activity in the liver of APAP-treated rats. Thus, *C. humilis* can effectively protect against APAP hepatotoxicity, pending additional investigations to figure out the underlying mechanism(s).

Conflict of Interests

The authors declare no conflict of interest.

Availability of data and materials

The manuscript and supplementary material contain all data supporting the reported results.

Acknowledgments

The authors extend their appreciation to the Researchers Supporting Project number (RSPD2024R628), King Saud University, Riyadh, Saudi Arabia for supporting this research.

Authors' Contributions:

Conceptualization: A.M.M. and E.M.K.; Methodology: S.A.A., A.M.M., H.M.D.N., H.M.H., M.M.A., M.E.R., W.G.H., and S.A.A.; Investigation: S.A.A., A.M.M., H.M.D.N., H.M.H., M.M.A., M.E.R., W.G.H., and S.A.A.; Data curation: A.M.M., E.M.K., and S.A.A.; Formal analysis: A.M.M., and E.M.K.; Validation: E.M.K.; Supervision: A.M.M., and E.M.K.; Writing-Original draft: A.M.M., E.M.K.; Writing-review and editing: A.M.M.

References:

[1] aJ. Kang, K. M. Thakali, C. Xie, M. Kondo, Y. Tong, B. Ou, G. Jensen, M. B. Medina, A. G. Schauss, X. Wu, *Food Chemistry* **2012**, *133*, 671-677; bW. Kchaou, F. Abbès, R. B. Mansour, C. Blecker, H. Attia, S. Besbes, *Food Chem* **2016**, *194*, 1048-1055; cS. Gonçalves, J. Medronho, E. Moreira, C. Grosso, P. B. Andrade, P. Valentão, A. Romano, *3 Biotech* **2018**, *8*, 88.

[2] aH. N. Gad El-Hak, H. S. Mahmoud, E. A. Ahmed, H. M. Elnegris, T. S. Aldayel, H. M. A. Abdelrazek, M. T. A. Soliman, M. A. I. El-Menyawy, *Nutrients* **2022**, *14*; bA. I. Hamed, R. Ben Said, A. S. Al-Ayed, J. Moldoch, U. A. Mahalel, A. M. Mahmoud, H. A. Elgebaly, A. J. Perez, A. Stochmal, *Nat Prod Res* **2017**, *31*, 2024-2031.

[3] J. M. Fedriani, M. J. E. Delibes, **2011**, *92*, 304-315.

[4] A. Giovino, S. Scibetta, S. Saia, C. Guarino, *Botanical Journal of the Linnean Society* **2014**, *176*, 66-81.

[5] I. Hinad, Y. S'Hih, A. Elhessni, A. Mesfioui, M. L. Ouahidi, *Pan Afr Med J* **2022**, *42*, 319.

[6] aJ. C. Caissard, A. Meekijjironenroj, S. Baudino, M. C. J. A. J. o. B. Anstett, **2004**, *91*, 1190-1199; bA. Bouhafsoun, M. A. Yilmaz, A. Boukeloua, H. Temel, M. K. J. F. S. HARCHE, Technology, **2018**, *38*, 242-247; cY. Hirai, S. SANADA, Y. IDA, J. J. C. SHOJI, p. bulletin, **1986**, *34*, 82-87.

[7] M. Miguel, S. Aazza, F. Gaamoussi, N. Bouchmaa, B. Lyoussi, *Fresenius Environmental Bulletin* **2014**, *23*, 1375-1388.

[8] aR. S. Alruhaimi, G. Mostafa-Hedeab, M. S. Abduh, A. Bin-Ammar, E. H. M. Hassanein, E. M. Kamel, A. M. Mahmoud, *Front Pharmacol* **2023**, *14*, 1204641; bM. O. Germoush, A. M. Mahmoud, *J Cancer Res Clin Oncol* **2014**, *140*, 1103-1109; cA. M. Mahmoud, O. A. M. Abd El-Ghafar, M. A. Alzoghaibi, E. H. M. Hassanein, *Life Sci* **2021**, *278*, 119600; dA. M. Mahmoud, W. G. Hozayen, I. H. Hasan, E. Shaban, M. Bin-Jumah, *Inflammation* **2019**, *42*, 1103-1116; eA. Fadel, A. M. Mahmoud, J. J. Ashworth, W. Li, Y. L. Ng, A. Plunkett, *International Journal of Biological Macromolecules* **2018**, *109*, 819-831; fA. Abdel-Moneim, B. M. Morsy, A. M. Mahmoud, M. A. Abo-Seif, M. I. Zanaty, *EXCLI Journal* **2013**, *12*, 943-955.

[9] K. Du, A. Ramachandran, H. Jaeschke, *Redox Biol* **2016**, *10*, 148-156.

[10] H. Jaeschke, *J Pharmacol Exp Ther* **1990**, *255*, 935-941.

[11] M. Frisch, G. Trucks, H. Schlegel, G. Scuseria, M. Robb, J. Cheeseman, G. Scalmani, V. Barone, B. Mennucci, G. J. G. I. Petersson, Wallingford, CT, **2009**.

[12] aA. D. Becke, *The Journal of Chemical Physics* **1993**, *98*, 5648-5652; bC. Lee, W. Yang, R. G. Parr, *Physical review B* **1988**, *37*, 785; cA. D. Becke, *Physical review A* **1988**, *38*, 3098.

[13] W. J. Hehre, L. Radom, P. v. R. Schleyer, J. A. Pople, *Ab initio molecular orbital theory, Vol. 67*, Wiley New York et al., **1986**.

[14] E. F. Pettersen, T. D. Goddard, C. C. Huang, G. S. Couch, D. M. Greenblatt, E. C. Meng, T. E. Ferrin, *Journal of computational chemistry* **2004**, *25*, 1605-1612.

[15] O. Trott, A. J. Olson, *Journal of computational chemistry* **2010**, *31*, 455-461.

[16] E. M. Kamel, A. M. Lamsabhi, *Organic & Biomolecular Chemistry* **2020**, *18*, 3334-3345.

[17] J. Cheel, C. Theoduloz, J. A. Rodríguez, P. D. Caligari, G. Schmeda-Hirschmann, *Food Chem.* **2007**, *102*, 36-44.

[18] M. Ozyürek, B. Bektaşoğlu, K. Güçlü, R. Apak, *Anal. Chim. Acta* **2009**, *636*, 42-50.

[19] D. K. Chellappan, S. Ganasen, S. Batumalai, M. Candasamy, P. Krishnappa, K. Dua, J. Chellian, G. Gupta, *Recent Pat Drug Deliv Formul* **2016**, *10*, 72-76.

[20] S. A. Mard, K. Jalalvand, M. Jafarinejad, H. Balochi, M. K. Naseri, *Malays J Med Sci* **2010**, *17*, 4-13.

[21] J. D. Bancroft, M. Gamble, *Theory and practice of histological techniques*, Elsevier health sciences, **2008**.

[22] M. N. Islam, I. J. Ishita, H. A. Jung, J. S. Choi, *Food and Chemical Toxicology* **2014**, *69*, 55-62.

[23] J. Jiao, Y. Zhang, C. Liu, J. e. Liu, X. Wu, Y. J. J. o. A. Zhang, F. Chemistry, **2007**, *55*, 10086-10092.

[24] aR. H. Elsayed, E. M. Kamel, A. M. Mahmoud, A. A. El-Bassuony, M. Bin-Jumah, A. M. Lamsabhi, S. A. J. F. Ahmed, C. Toxicology, *Journal of food and chemical toxicology* **2020**, *138*, 111202; bJ.-H. Yang, T. P. Kondratyuk, L. E. Marler, X. Qiu, Y. Choi, H. Cao, R. Yu, M. Sturdy, S. Pegan, Y. J. P. Liu, **2010**, *71*, 641-647.

[25] M. Yoshikawa, F. Xu, T. Morikawa, Y. Pongpiriyadacha, S. Nakamura, Y. Asao, A. Kumahara, H. J. C. Matsuda, P. bulletin, **2007**, *55*, 308-316.

[26] T. Nakanishi, M. Kobayashi, H. Murata, A. J. C. Inada, p. bulletin, **1988**, *36*, 4148-4152.

[27] I. Ahmad, F. Ahmad, S. J. P. Osman, **1977**, *16*, 1761-1763.

[28] J. U. Obaroakpo, L. Liu, S. Zhang, L. Jing, L. Liu, X. Pang, J. J. J. o. F. F. Lv, **2020**, *66*, 103779.

[29] M. Prabakaran, S.-H. Kim, A. Sasireka, V. Hemapriya, I.-M. J. N. J. o. C. Chung, **2017**, *41*, 3900-3907.

[30] J. M. Choi, E. O. Lee, H. J. Lee, K. H. Kim, K. S. Ahn, B. S. Shim, N. I. Kim, M. C. Song, N. I. Baek, S. H. J. P. R. Kim, **2007**, *21*, 954-959.

[31] D. S. Budnitz, M. C. Lovegrove, A. E. Crosby, *Am J Prev Med* **2011**, *40*, 585-592.

[32] A. M. Mahmoud, M. Y. Alexander, Y. Tutar, F. L. Wilkinson, A. Venditti, *Oxid Med Cell Longev* **2017**, *2017*, 2508909.
[33] N. Malik, P. Dhiman, E. Sobarzo-Sanchez, A. Khatkar, *Curr. Top. Med. Chem.* **2018**, *18*, 2154-2164.
[34] aO. Dangles, *Curr. Org. Chem.* **2012**, *16*, 692-714; bE. M. Kamel, A. Bin-Ammar, A. A. El-Bassuony, M. M. Alanazi, A. Altharawi, A. F. Ahmeda, A. S. Alanazi, A. M. Lamsabhi, A. M. Mahmoud, *RSC Advances* **2023**, *13*, 12361-12374.
[35] aE. M. Kamel, A. M. Lamsabhi, *Organic & Biomolecular Chemistry* **2021**, *19*, 9031-9042; bE. M. Kamel, A. M. Tawfeek, A. A. El-Bassuony, A. M. Lamsabhi, *New Journal of Chemistry* **2023**.
[36] aE. M. Kamel, N. A. Ahmed, A. A. El-Bassuony, O. E. Hussein, B. Alrashdi, S. A. Ahmed, A. M. Lamsabhi, H. H. Arab, A. M. Mahmoud, *J Combinatorial Chemistry and High Throughput Screening* **2022**, *25*, 1336-1344; bE. M. Kamel, A. M. Tawfeek, A. A. El-Bassuony, A. M. Lamsabhi, *Organic & Biomolecular Chemistry* **2023**.
[37] B. M. ALRashdi, H. A. Elgebaly, M. O. Germoush, M. M. Qarmush, M. S. Azab, R. S. Alruhaimi, A. F. Ahmeda, M. H. Abukhalil, E. M. Kamel, H. H. J. E. S. Arab, P. Research, *Environmental Science and Pollution Research* **2022**, *in press*, 1-13.
[38] aİ. Ö. Aycan, A. Tüfek, O. Tokgöz, O. Evliyaoğlu, U. Fırat, G. Ö. Kavak, H. Turgut, M. U. Yüksel, *International Journal of Surgery* **2014**, *12*, 213-218; bA. Mohammadi, S. Kazemi, M. Hosseini, H. Najafzadeh Varzi, F. Feyzi, P. Morakabati, A. A. Moghadamnia, *Chemical Research in Toxicology* **2019**, *32*, 2329-2337; cP. Hasanein, M. Sharifi, *Pharmaceutical Biology* **2017**, *55*, 1809-1816; dA. Rajasekaran, M. Periyasamy, *Chinese Medicine* **2012**, *7*, 12.
[39] H. Jaeschke, M. R. McGill, A. Ramachandran, *Drug Metab Rev* **2012**, *44*, 88-106.
[40] M. S. Abduh, M. A. Alzoghaibi, A. M. Alzoghaibi, A. Bin-Ammar, M. F. Alotaibi, E. M. Kamel, A. M. Mahmoud, *Life Sci* **2023**, 121612.
[41] A. Wendel, S. Feuerstein, K. H. Konz, *Biochem Pharmacol* **1979**, *28*, 2051-2055.
[42] A. Wendel, S. Feuerstein, *Biochem Pharmacol* **1981**, *30*, 2513-2520.
[43] aM. S. Abduh, S. A. M. Saghir, A. M. Al Hroob, A. Bin-Ammar, A. H. Al-Tarawni, V. Murugaiyah, A. M. Mahmoud, *Front Pharmacol* **2023**, *14*, 1134812; bA. M. Abdul-Rahman, A. Elwekeel, R. S. Alruhaimi, E. M. Kamel, A. Bin-Ammar, A. M. Mahmoud, A. S. Moawad, M. A. Zaki, *Saudi Pharmaceutical Journal* **2023**, *31*, 101762.

Tables:

Table1. Binding affinities, polar bonds, and hydrophobic interactions of phytochemicals (**1**-**11**) isolated from *C. humilis* with XO.

	Xanthine oxidase		
	Affinity (kcal/mol)	Polar bonds	Hydrophobic interactions
1	-9.7	Phe798, Arg912, Met1038, Thr1077, Ser1080, Gln1194, Val1259 and Val1260	Gln585, Tyr592, Leu744, Gly795, Gly796, Gly1039, Gln1040, Leu1042, Ala1078, Ser1082 and Thr1083
2	-7.2	Leu648, Asn768, His875 and Ser876	Phe649, Lys771, Val1011, Phe1013, Leu1013 and Pro1076
3	-8.4	Arg912, Lys1045, Ser1082 and Thr1083	Gln767, Phe798, Gly799, Glu802, Gln1040, Ala1078, Ala1079, Ser1080, Gln1194, Val1259, Gly1260 and Glu1261
4	-7.7	Ile698, Glu699, Glu1210, Leu1211, His1212 and Tyr1213	Ile696, Thr697, Tyr735, Leu843 and Lys 1304
5	-7.6	Lys713, Phe1142 and Glu1143	Glu711, Leu712, His875, Glu879, Pro1012, Gly1139 and Tyr1140
6	-7.3	His741 and Gln1201	Val1200, Ile1229, Pro1230 and Ile1235
7	-8.7	Phe798, Gly1039, Ala1079, Ser1080, Gly1139 and Gln1194	His741, Phe742, Gly797, Arg912, Met1038, Gln1040, Ala1078, Gly1197, Val1200, Gln1201 and Glu1261
8	-6.4	Arg912 and Gln1194	His741, Phe798, Met1038, Gly1038, Gln1040, Gly1197, Gln1201, Glu1209, Pro1230 and Ile1229
9	-8.3	Arg912	Gln585, Leu744, Gly795, Phe798, Gly1197, Gln1201, Ile1229 and Pro1230
10	-7.0	Gly1039	Phe798, Arg912, Gln1194, Gly1197, Val1200, Gln1201, Ile1129, Pro1230, Ala1231 and Phe1232
11	-7.1	--	Phe742, Leu744, Gly795, Phe798, Met1038, Gly1039, Gln1194, Gly1197, Val1200, Gln1201, Ile1229 and Pro1230

Figures:

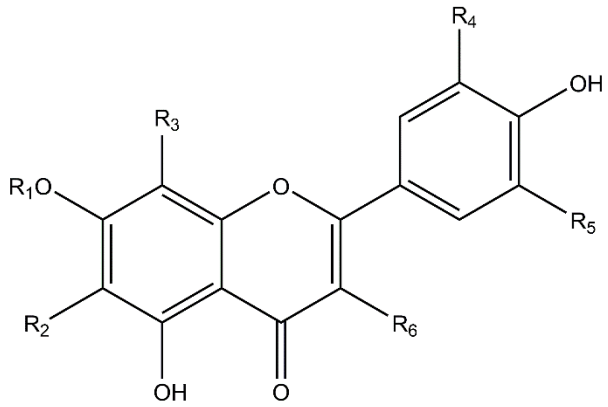

1 R1 = rutinoside, R2 = H, R3 = H, R4 = OMe, R5 = OMe and R6 = H

2 R1 = H, R2 = *C*-glucopyranoside, R3 = *C*-glucopyranoside, R4 = H, R5 = H and R6 = H

3 R1 = H, R2 = H, R3 = H, R4 = OMe, R5 = OMe and R6 = H

4 R1 = H, R2 = H, R3 = H, R4 = H, R5 = H and R6 = *O*-*β*-D-glucopyranoside

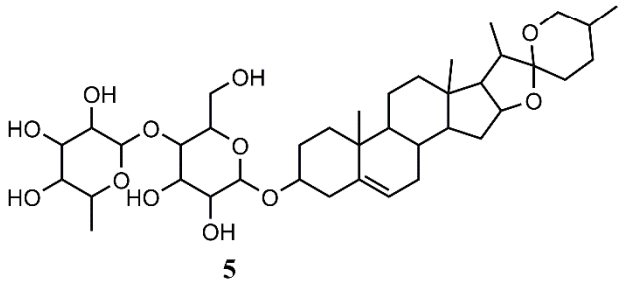

5

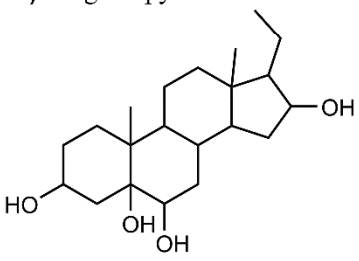

6

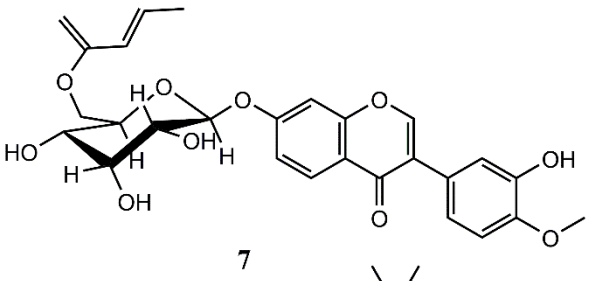

7

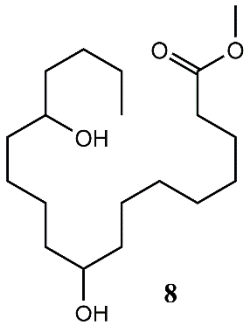

8

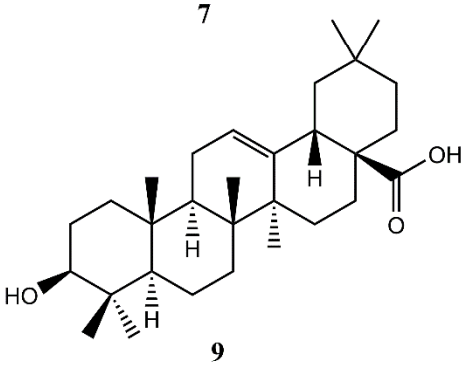

9

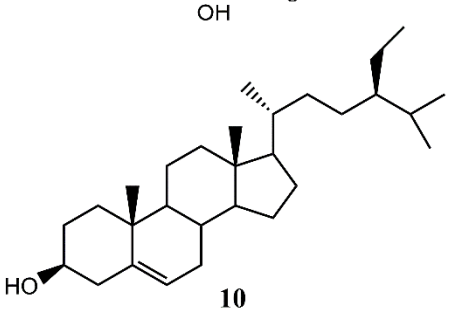

10

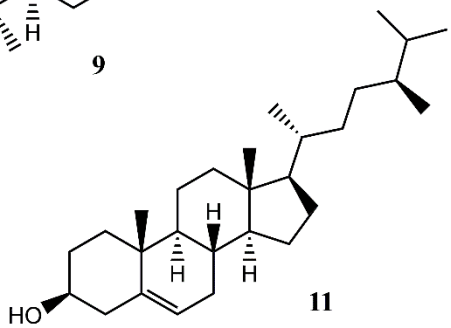

11

Fig. 1. Chemical structure of the compounds isolated from different fractions of *C. humilis*.

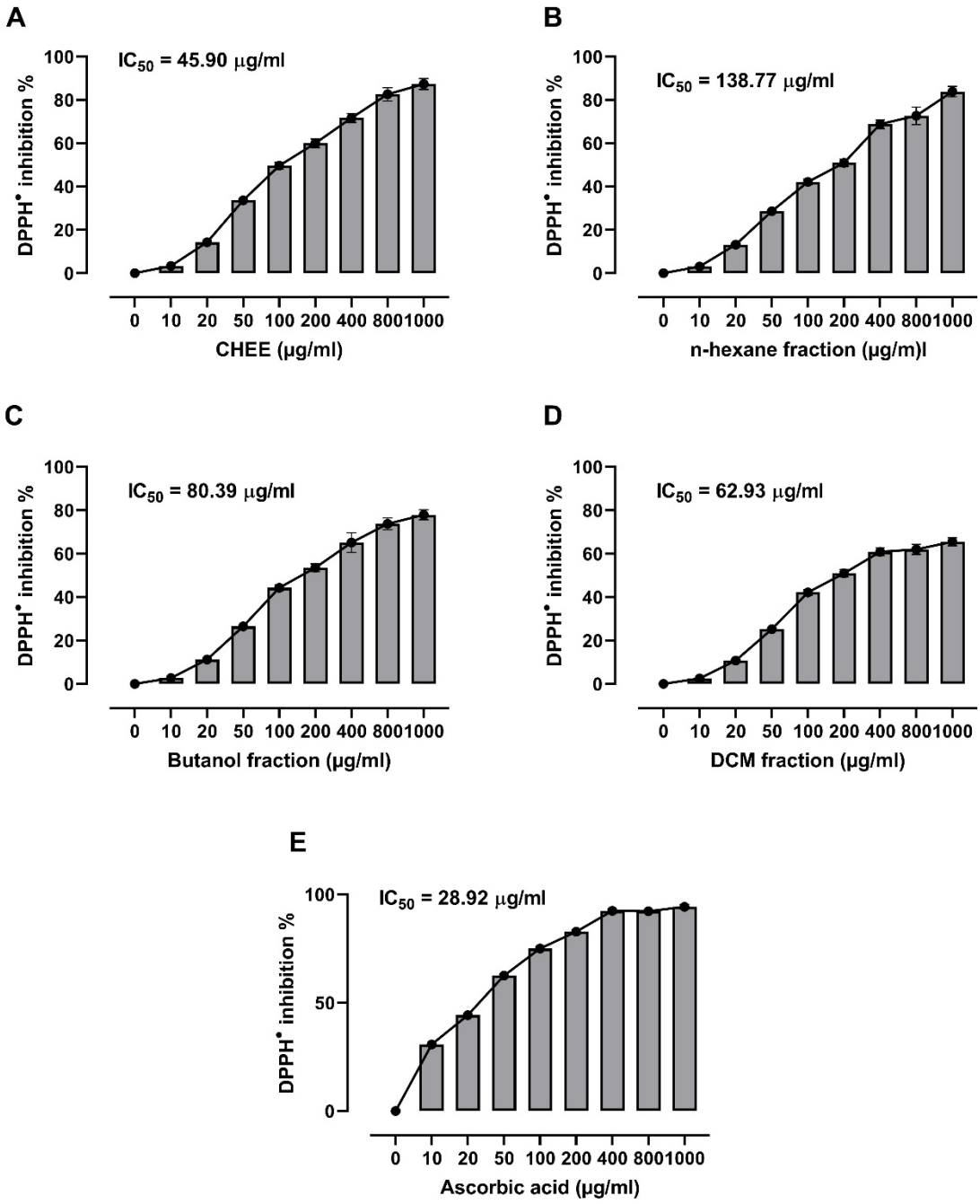

487

488 Fig. 2. DPPH radical scavenging activity and IC50 values of *C. humilis* leaves ethanolic extract
489 (CHEE) and its fractions, and ascorbic acid. Data are mean ± SD, (N=3).

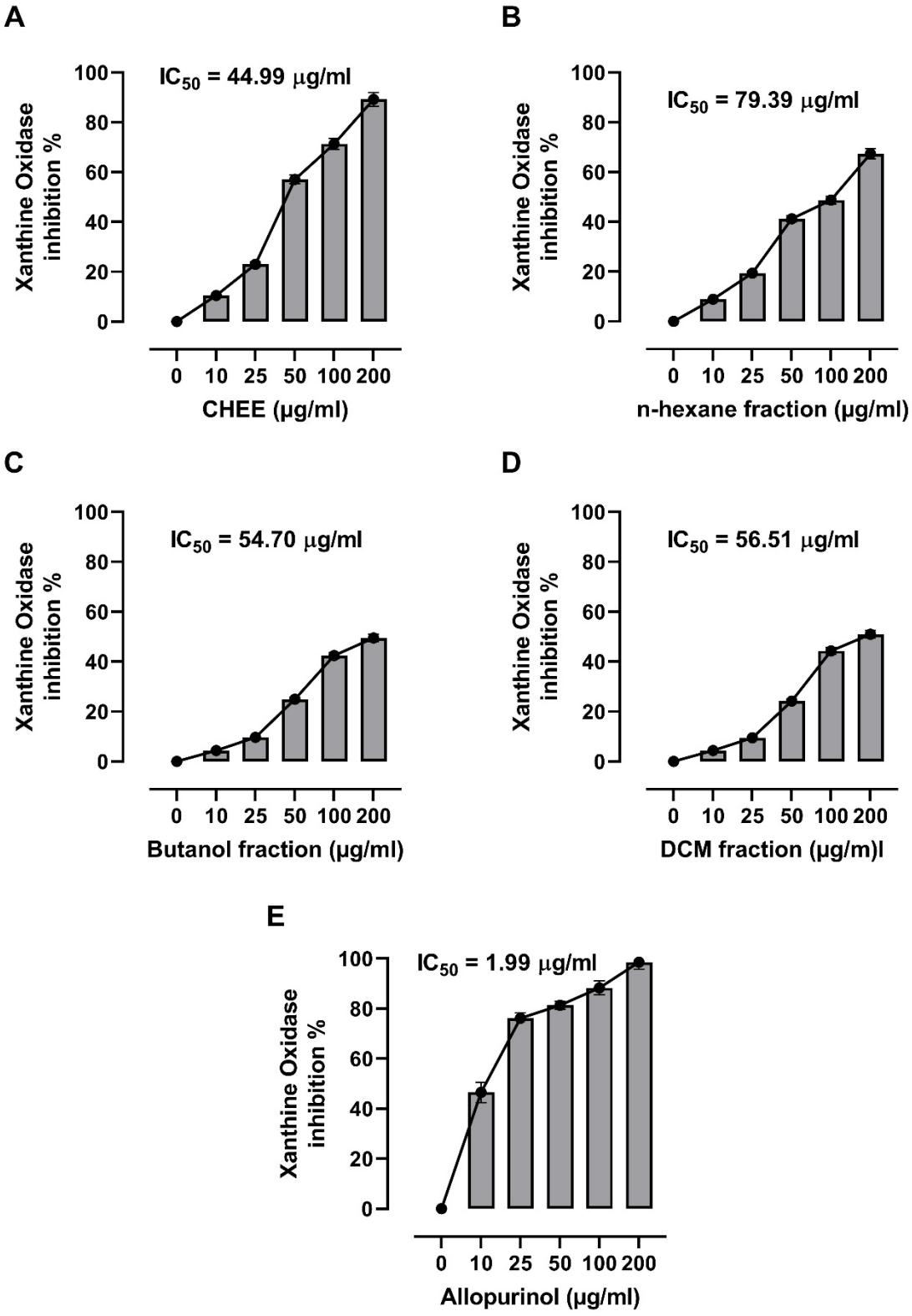

490

491 Fig. 3. XO inhibitory activity and IC50 values of *C. humilis* leaves ethanolic extract (CHEE)
492 and its fractions, and ascorbic acid. Data are mean ± SD, (N=3).

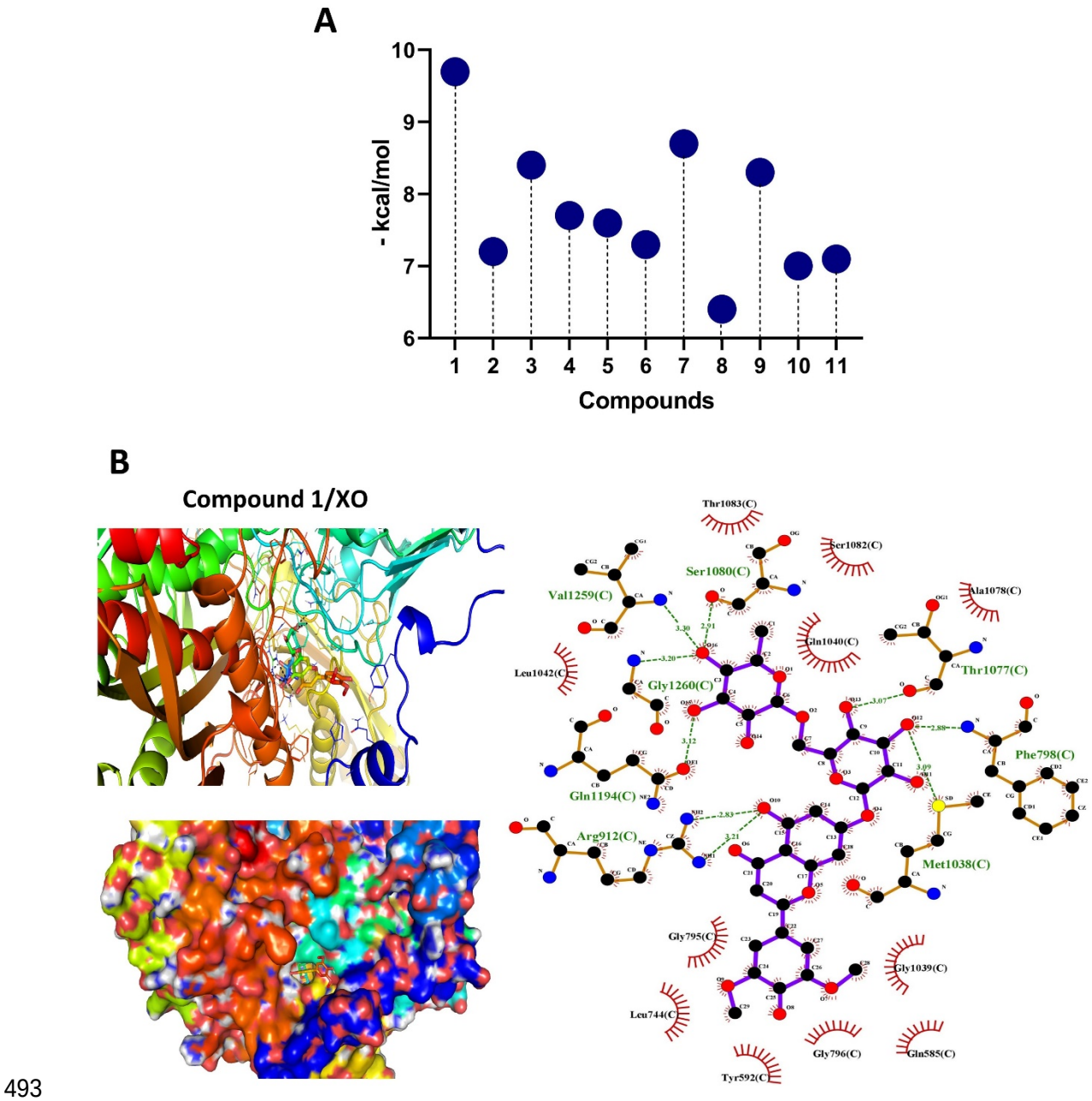

493

494 Fig. 4. The lowest binding energies of the compounds isolated from different fractions of *C.*
495 *humilis* with XO (A) and molecular docking simulation of compound **1** with XO (B).

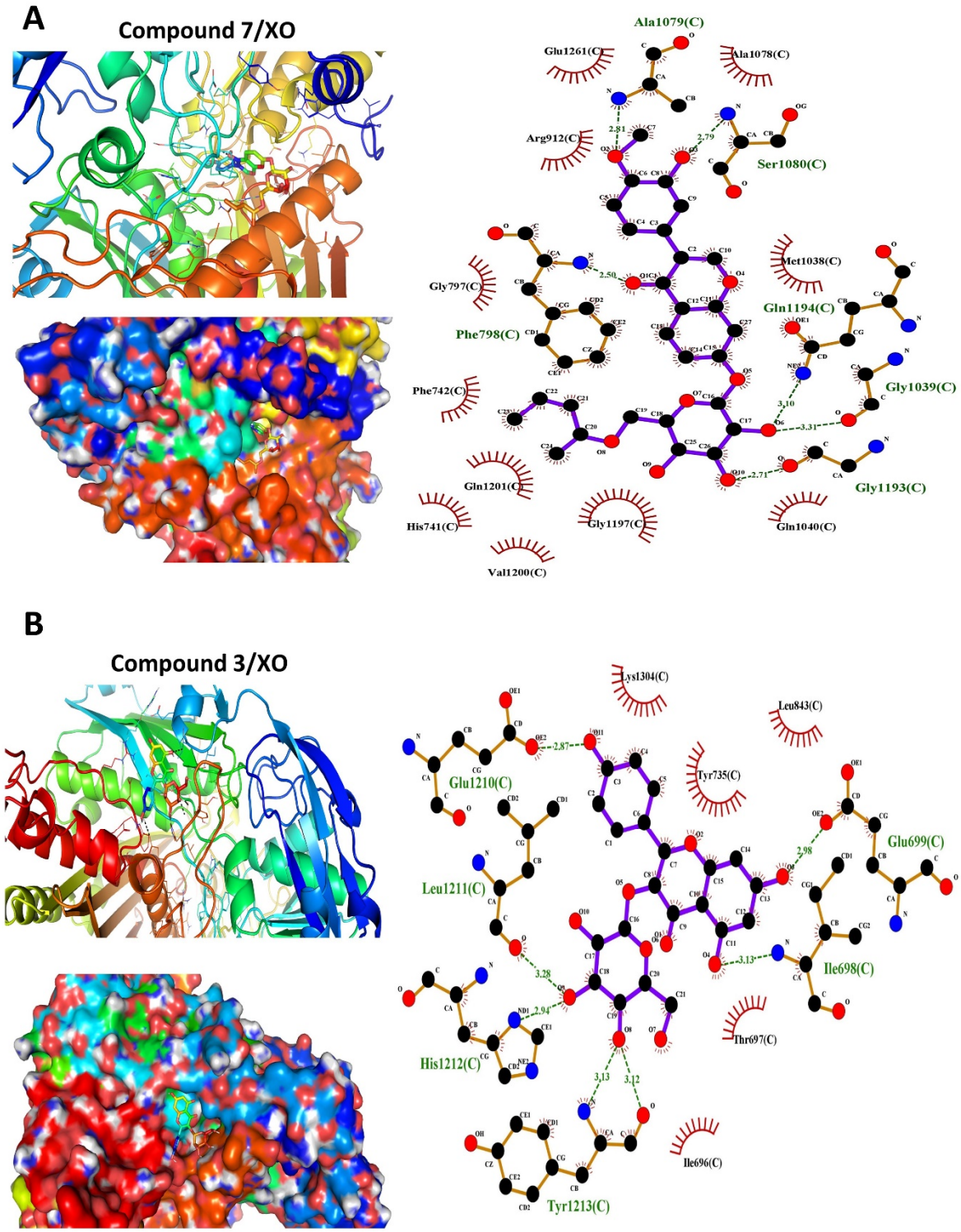

Fig. 5. Molecular docking simulation of compounds **7** (A) and **3** (B) isolated from *C. humilis* with XO.

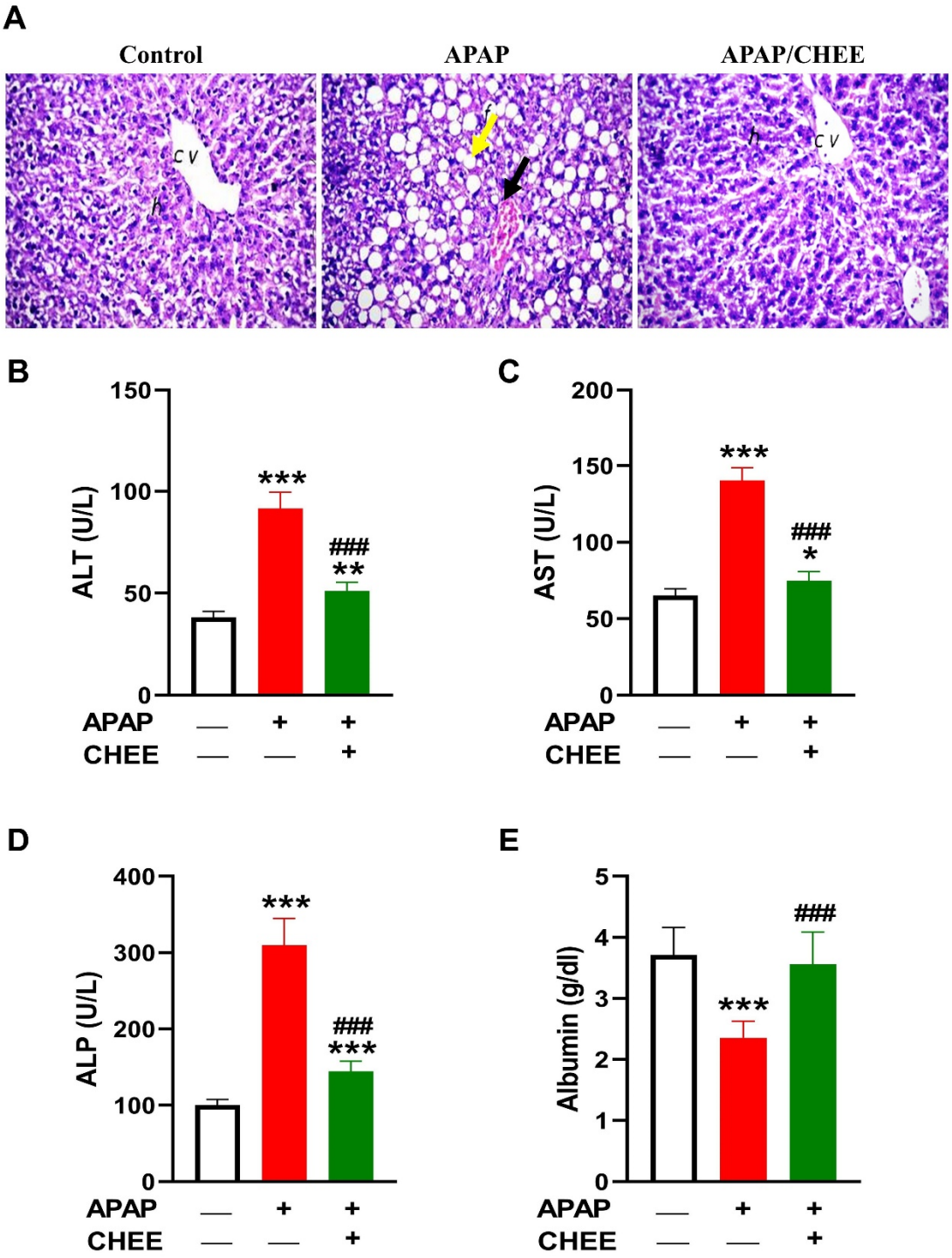

500

501 Fig. 6. *C. humilis* ethanolic extract (CHEE) ameliorated APAP-hepatotoxicity in rats. (A)
502 Photomicrographs of H&E-stained sections (X400) in the liver of control rats showing normal
503 histological architecture, APAP-administered rats showing hydropic degeneration (yellow
504 arrow) and hemorrhage (black arrow), and APAP-administered rats treated with CHEE
505 showing nearly normal liver tissue architecture without vacuolations or hemorrhages. (B-E)
506 CHEE decreased ALT (B), AST (C) and ALP (D) activities and increased albumin (E) in serum

of APAP-administered rats. Data are mean ± SEM, (n = 6). *P<0.05, **P<0.01 and ***P<0.001 vs Control, and ###P<0.001 vs APAP.

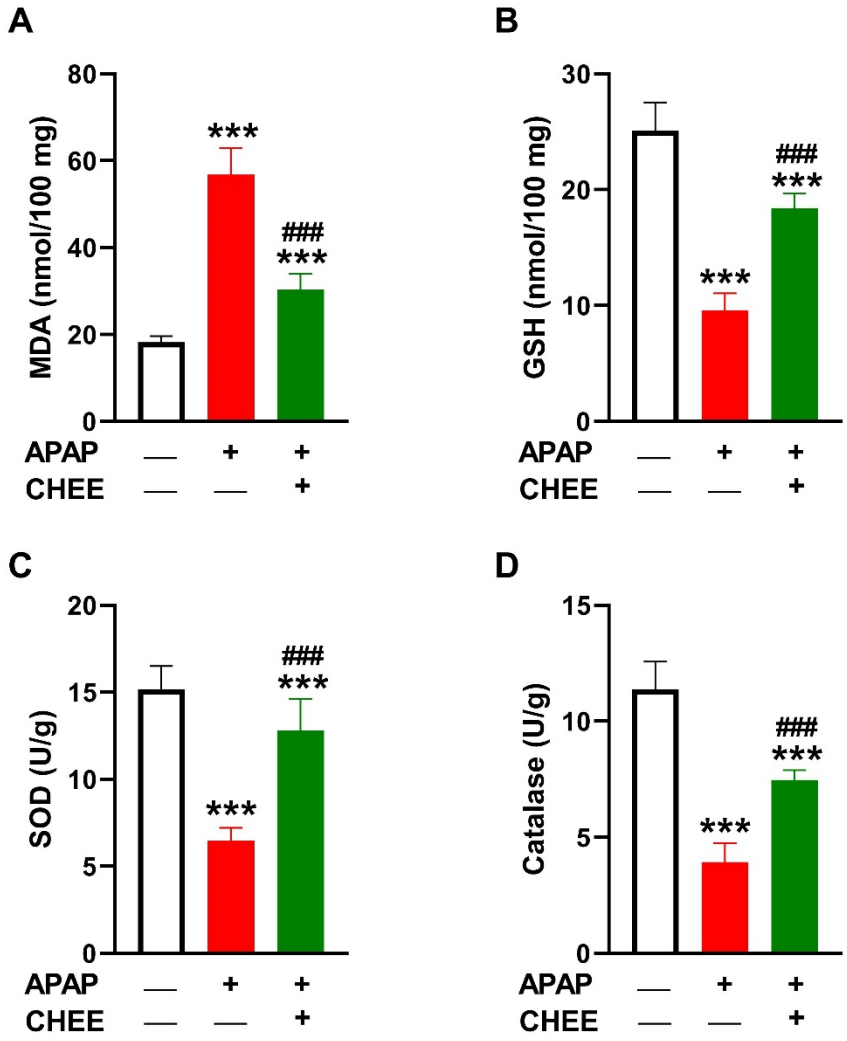

Fig. 7. *C. humilis* ethanolic extract (CHEE) attenuated APAP-induced oxidative stress in liver of rats. CHEE decreased MDA (A) and increased GSH (B), SOD (C) and catalase (D). Data are mean ± SEM, (n = 6). ***P<0.001 vs Control, and ###P<0.001 vs APAP.

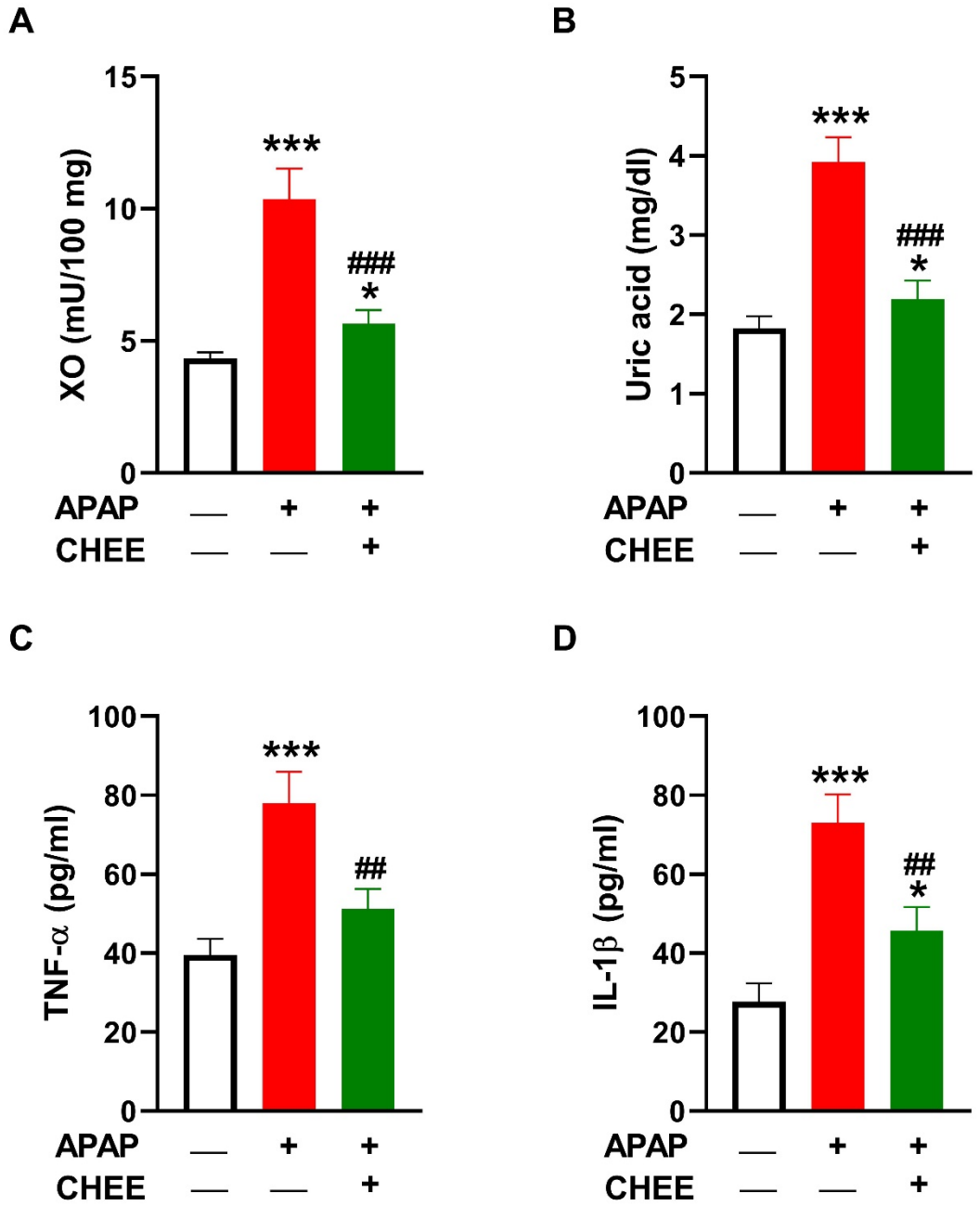

513

514 Fig. 8. *C. humilis* ethanolic extract (CHEE) decreased liver XO (A), and serum uric acid (B),
515 TNF-α (C) and IL-1β (D) in APAP-administered rats. Data are mean ± SEM, (n = 6). *P<0.05
516 and ***P<0.001 vs Control. ##P<0.01 and ###P<0.001 vs APAP.